



Removal of azo and anthraquinone reactive dyes from industrial wastewaters using MgO nanoparticles

Gholamreza Moussavi*, Maryam Mahmoudi

Department of Environmental Health, School of Medical Sciences, Tarbiat Modares University, Tehran, Iran

ARTICLE INFO

Article history:

Received 20 May 2008

Received in revised form 22 October 2008

Accepted 17 February 2009

Available online 25 February 2009

Keywords:

Dye removal

Azo and anthraquinone dye

Reactive blue 19

Reactive red 198

Adsorption

ABSTRACT

In the present investigation, a porous MgO powder was synthesized and tested for the removal of dyes from aqueous solution. The size of the MgO particles was in the range of 38–44 nm, with an average specific surface area of 153.7 m²/g. Adsorption of reactive blue 19 and reactive red 198 was conducted to model azo and anthraquinone dyes at various MgO dosages, dye concentrations, solution pHs and contact times in a batch reactor. Experimental results indicate that the prepared MgO powder can remove more than 98% of both dyes under optimum operational conditions of a dosage of 0.2 g, pH 8 and a contact time of 5 min for initial dye concentrations of 50–300 mg/L. The isotherm evaluations revealed that the Langmuir model attained better fits to the experimental equilibrium data than the Freundlich model. The maximum predicted adsorption capacities were 166.7 and 123.5 mg of dye per gram of adsorbent for RB 19 and RR 198, respectively. In addition, adsorption kinetic data followed a pseudo-second-order rate for both tested dyes.

© 2009 Elsevier B.V. All rights reserved.

1. Introduction

According to the Color Index (C.I.), which is managed by the Society of Dyers and Colorists and the American Association of Textile Chemists and Colorists, currently more than 10,000 various types of dyes are synthesized and available in the world. Although no recent data is available on worldwide dye production, annual production of over 700,000 tonnes has been often reported in the literature [1–3]. Dyes are organic compounds consisting of two main groups of compounds, chromophores (responsible for color of the dye) and auxochromes (responsible for intensity of the color) [4]. Dyes are classified according to the chemical structure and type of application. Based on chromophores, 20–30 different groups of dyes can be discerned, with azo, anthraquinone, phthalocyanine and triaryl-methane accounting for the most important groups. Azo (around 70%) and anthraquinone (around 15%) compose the largest classes of dyes.

Many industries, such as dyestuffs, textile, paper and plastics, use dyes to color their products; as a result, these industries produce color-containing wastewater as an unavoidable by-product [3,5]. It is estimated that around 10–15% of dyes are wasted into the environment upon completion of their use in the dyeing unit. One

of the most important industries using dyes is the textile industry [6], which generates a strongly colored wastewater, typically with a concentration in the range of 10–200 mg/L [7,8].

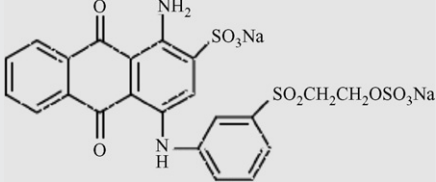
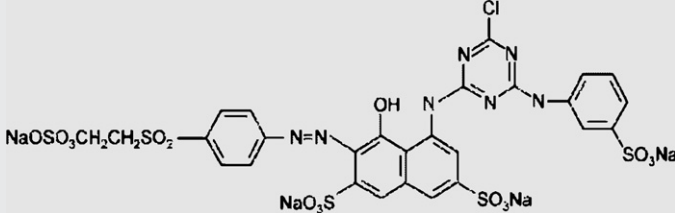
Since dyes are stable, recalcitrant, colorant, and even potentially carcinogenic and toxic [9,10], their release into the environment poses serious environmental, aesthetic and health problems. Thus, industrial dye-laden effluents are an increasingly major concern and need to be effectively treated before being discharged into the environment in order to prevent these potential hazards.

Many investigations have reported methods for the removal of dyes from water and wastewater using various methods, including biological processes, combined chemical and biochemical processes, chemical oxidation, adsorption, coagulation and membrane treatments; each of these has specific advantages and disadvantages. Reviewing the available literature indicated that the adsorption is one of the most investigated techniques for dye removal. This is likely due to its simplicity and high level of effectiveness [11]. Several types of natural and synthetic adsorbents have been evaluated for the removal of dyes from colored water and wastewater [5,12–14]. Among these materials, activated carbon is one of the most widely studied and used adsorbents for environmental pollution control. The main disadvantage of activated carbon is its high production and treatment costs [12,15]. Thus, many researchers throughout the world have focused their efforts on optimizing adsorption and developing novel alternative adsorbents with high adsorptive capacity and low cost. In this regard, much attention has recently been paid to nanotechnology. Several articles have been published on the application of

* Corresponding author at: Department of Environmental Health, School of Medical Sciences, Tarbiat Modares University, P.O. Box 14115-331, Tehran, Iran. Tel.: +98 21 82883827.

E-mail address: Moussavi@modares.ac.ir (G. Moussavi).

Table 1
Basic properties of the investigated dyes.

Characteristic	RB 19	RR 198
Chemical formula	C ₂₂ H ₁₆ O ₁₁ N ₂ S ₃ Na ₂	C ₂₇ H ₁₈ ClN ₇ Na ₄ O ₁₅ S ₅
Commercial name	Remazol Brilliant Blue R	Remazol Red 133
Class	Anthraquinone	Azo
C.I. number	61200	18221
Molecular weight (g/mol)	626.5	967.5
λ _{max} (nm)	592	518
Molecular structure		

various nanoparticles for the treatment and remediation of pollutants in the environment [16–18], some even focusing specifically on dye removal [19–21]. Nano-materials have large specific surface areas, and thus a large fraction of atoms are available for chemical reaction. Nano-sized alkaline earth metal oxides, in particular magnesium oxide (MgO), are very promising materials for applications as adsorbents due to their destructive sorbent [16,22], high surface reactivity and adsorption capacity compared to their commercial analogues [23], and the simplicity of their production from abundant natural minerals. Furthermore, as the pH of zero point charge (pH_{ZPC}) of MgO is 12.4 [24], it is a suitable adsorbent for the adsorption of anions due to its favorable electrostatic attraction mechanism.

The present study focuses on the preparation of MgO nanoparticle and investigations into its efficiency as an adsorbent for the removal of azo and anthraquinone dyes from wastewater. Reactive blue 19 (RB 19) and reactive red 198 (RR 198) were taken as models for azo and anthraquinone dyes, respectively, for removal investigation. The effect of different variables, including dosage of MgO, concentration of dye, pH of the liquid and reaction time, on removal of the two model dyes was evaluated. Adsorption isotherms and kinetics were also analyzed.

2. Experimental

2.1. Chemicals and reagents

The model textile reactive dyes were purchased from the commercial manufacturing company DyStar Co. (Germany). Some of the important physicochemical properties of the investigated dyes are given in Table 1. All chemicals and reagents used were analytical grade, and distilled water was used in the preparation of solutions in the present investigation. The 2% stock liquid dye solutions from each dye were prepared by dissolving a known amount of the dye in 1 L of distilled water. For treatment experiments, the dye solutions with concentrations in the range of 50–300 mg/L were prepared by successive dilution of the stock solution with distilled water.

2.2. Preparation of MgO nanoparticles

MgO nanoparticles are usually synthesized by hydrothermal or sol-gel techniques [16,25–27]. In this experiment, nano-MgO was synthesized by the sol-gel method. To prepare nanoparticles of MgO, 100 g of MgCl₂·6H₂O was first dissolved in 500 mL of distilled water in a 1-L beaker, into which 50 mL of 1N NaOH solution was added. The solution was then rapidly stirred for 4 h to generate the magnesium hydroxide precipitates. The suspension was cen-

trifuged at 3000 rpm for 5 min to obtain the Mg(OH)₂ gel, washed several times with distilled water and dried at 60 °C for 24 h. The dried powder was finally calcinated in air under 450 °C for 2 h and MgO nanoparticles were such made.

2.3. Dye removal experiments

Dye removal experiments with the synthesized MgO nanoparticles were carried out as batch tests in 250 mL flasks under magnetic stirring. The experiments were conducted individually for each of the model dyes, but the same procedure was used for both, as detailed below. Each test consisted of preparing a 100 mL of dye solution with a desired initial concentration and pH by diluting the stock dye solutions with distilled water, and transferring it into the beaker on the magnetic stirrer. The pH of the solution was adjusted using 0.1N HCl or NaOH solutions. A known mass of nano-MgO powder (MgO dosage) was then added to the solution, and the obtained suspension was immediately stirred for a predefined time. After the mixing time elapsed, the suspension was allowed to settle and the supernatant was analyzed for the residual dye. The adsorption percent of each of dye, i.e. the dye removal efficiency, was determined using the following expression:

$$\text{dye removal efficiency (\%)} = \frac{C_0 - C_f}{C_0} \times 100$$

where C₀ and C_f represent the initial and final (after adsorption) dye concentrations, respectively. All tests were performed in duplicate to insure the reproducibility of the results; the mean of the two measurements is reported. All experiments were performed at room temperature. The investigated ranges of the experimental variables were as follows: dye concentration (50–300 mg/L), pH of solution (3–12), MgO dosage (0.05–1 g) and mixing time (1–20 min).

2.4. Adsorption isotherms

The equilibrium isotherm of a specific adsorbent represents its adsorptive characteristics and is very important to the design of adsorption processes [28]. Experiments for the estimation of the adsorption isotherms of RB 19 and RR 198 onto MgO nanoparticles were performed by adding various quantities of MgO powder, in the range of 0.05–1 g, to a series of Erlenmeyer flasks, each containing 100 mL of dye solution with a concentration of 100 mg/L and pH of 8. The vessels were then stirred for 48 h at constant-temperature (25 °C) to attain equilibrium, after which time the settled solutions were analyzed for concentration of the residual dye. This experiment was carried out for both the dyes individually. The amount of

dye adsorbed onto MgO nanoparticles was calculated based on the following mass balance equation:

$$q_e = \frac{V(C_0 - C_e)}{m}$$

where q_e is the adsorption capacity (mg dye adsorbed onto the mass unit of MgO, mg/g), V is the volume of the dye solution (L), C_0 and C_e (mg/L) are initial and equilibrium dye concentrations, and m (g) is the mass of dry MgO added.

The equilibrium relationship between the quantity of adsorbate per unit of adsorbent (q_e) and its equilibrium solution concentration (C_e) at a constant-temperature is known as the adsorption isotherm [29]. Developing an appropriate isotherm model for adsorption is essential to the design and optimization of adsorption processes [30]. Several isotherm models have been developed for evaluating the equilibrium adsorption of compounds from solutions such as Langmuir, Freundlich, Redlich–Peterson, Dubinin–Radushkevich, Sips, Temkin, etc. Since the more common models used to investigate the adsorption isotherm are Langmuir and Freundlich equations, the experimental results of this study were fitted with these two models.

The linearized form of the Langmuir isotherm, assuming monolayer adsorption on a homogeneous adsorbent surface, is expressed as follows [31]:

$$\frac{C_e}{q_e} = \frac{1}{bq_{\max}} + \frac{C_e}{q_{\max}}$$

where the q_{\max} (mg/g) is the surface concentration at monolayer coverage and illustrates the maximum value of q_e that can be attained as C_e is increased. The b parameter is a coefficient related to the energy of adsorption and increases with increasing strength of the adsorption bond. Values of q_{\max} and b are determined from the linear regression plot of (C_e/q_e) versus C_e . The Freundlich equation [32] is expressed as follows in its linearized form:

$$\log q_e = \log K_F + \frac{1}{n} \log C_e$$

where K_F and n are constants from the Freundlich equation. The constant K_F represents the capacity of the adsorbent for the adsorbate, and $1/n$ is the reciprocal of reaction order which is a function of the strength of adsorption. A linear regression plot of $\log q_e$ versus $\log C_e$ gives the K_F and n values.

2.5. Adsorption kinetics

Several models are available to investigate the adsorption mechanism and description based on experimental data. The pseudo-first- and pseudo-second-order reaction rate equations are the most commonly applied models among these [33]. The pseudo-first-order adsorption rate [33] and pseudo-second-order adsorption rate developed by Ho and McKay [34] have the following linear forms for boundary conditions of $q=0$ at $t=0$ and $q_t=q_e$ at $t=t_e$:

$$\text{pseudo-first-order equation : } \ln(q_e - q_t) = \ln q_e - k_1 t$$

$$\text{pseudo-second-order equation : } \frac{t}{q_t} = \frac{1}{k_2 q_e^2} + \frac{t}{q_e}$$

where k_1 and k_2 are constants of adsorption rate, q_t is adsorption capacity at time t , q_e is adsorption capacity at equilibrium condition.

2.6. Analysis

The synthesized powder was characterized for specific surface area, mean size and surface morphology of the particles. Specific surface area was determined by nitrogen sorption isotherm using

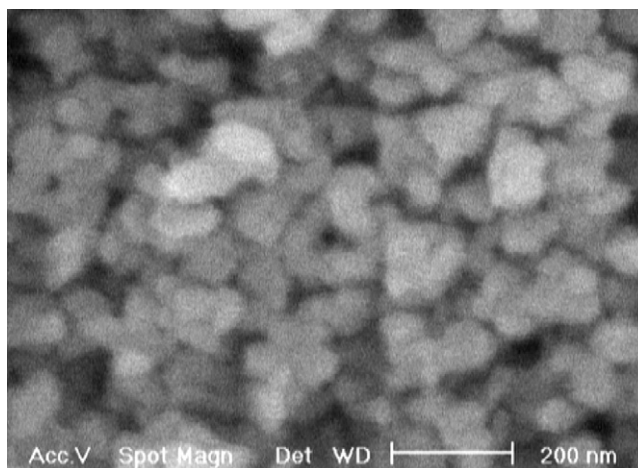


Fig. 1. The SEM image of MgO powder.

BET method [35]. The morphology of the particles was investigated using scanning electron microscopy (SEM) image. Samples of solutions before and after treatment were analyzed for the dyes using a UV–vis spectrophotometer (Unico-UV 2100) at their maximum absorption wavelengths (Table 1). The dye concentrations were calculated from the standard calibration curve obtained from standard dye solutions. The pH of the liquid samples was measured using a pH meter (Sense Ion 378, Hack).

3. Results and discussion

3.1. Characteristics of MgO nanoparticles

The surface and textural morphology of MgO powder by SEM image is illustrated in Fig. 1. According to the SEM image analysis, the size of MgO particles was found to range between 38 and 44 nm, which is greater than that reported by Nagappa and Chandrappa [16]. The specific surface area was determined using the BET equation applied to the adsorption data. The results of the BET method showed that the average specific surface area MgO nanoparticles was 103.5 m²/g. It can be concluded from these values that the MgO made is a nanoparticle with relatively large surface area.

3.2. Dye adsorption by MgO

The efficiency of the prepared and characterized MgO was investigated as an adsorbent for removal of RB 19 and RR 198 from liquid solutions. The experiments were performed under different experimental conditions. Results are presented in the following section.

3.2.1. Effect of MgO dosage

The effect of MgO quantity on removal of RB 19 and RR 198 was investigated in batch experiments by adding various amount of adsorbent in the range of 0.05–1 g powder into the flask containing 100 mL of dye solution. The initial dye concentrations and the pH of the solutions were fixed at 100 mg/L and 7, respectively, for all batch experiments. The suspension was then stirred for 20 min, after which time the solution was coagulated and settled and the supernatant was analyzed for the remaining dye. Results are shown in Fig. 2. As indicated, 36 and 36.4% of RB 19 and RR 198 were removed at the initial dosage of 0.05 g, respectively. The removal of both dyes increased with increasing MgO dosage up to 0.2 g and reached to over 99% for both RB 19 and RR 198 dyes at this dosage. This observation can be explained by the greater number of adsorption sites for dye molecules made available at greater MgO dosages [28,36]. Further increasing the adsorbent dose to 1 g did not affect

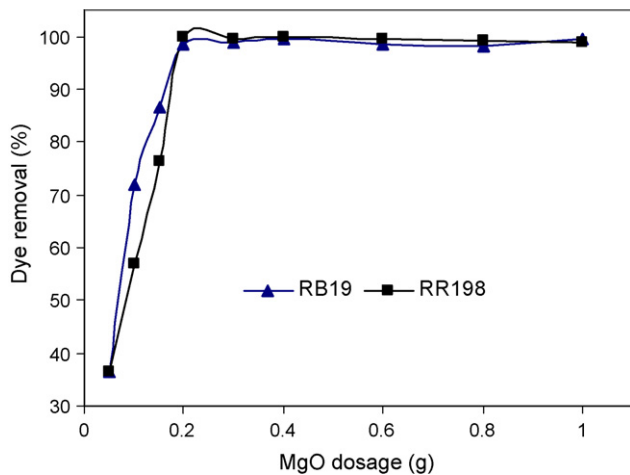


Fig. 2. Effect of initial dose of MgO on removal of RB 19 and RR 198 (initial pH 7, initial dye concentration = 100 mg/L, stirring time = 20 min).

the removal of any of both dyes. Hence, the optimum dosage of nano-MgO powder for removing both RB 19 and RR 198 was found to be 0.2 g. It was observed that, as long as sufficient adsorption sites are provided, the removal of RB 19 and RR 198 are independent of the adsorbent for MgO.

3.2.2. Effect of solution pH

Solution pH is an important parameter that affects adsorption of dye molecules. The effect of the initial pH of the solution on the RB 19 and RR 198 adsorption onto MgO powder was assessed at different values, ranging from 3 to 12, with a stirring time of 20 min. The initial concentrations of each dye and adsorbent dosage were set at 100 mg/L and 0.2 g, respectively, for all batch tests in this experiment. Fig. 3 presents the results of the effect of the solution pH on the RB 19 and RR 198 removal efficiencies. As shown in Fig. 3, removal of RB 19 increased from 86 to 100% when the pH was increased from 3 to 8. Since the removal of RB 19 increased to its maximum value at a pH of 8, the electrostatic attraction between the dye molecules (negatively charged) and MgO surface (positively charged; pH_{zpc} 12.4) might be the predominant adsorption mechanism [37]. If this were true, increasing solution pH would result in increasing adsorption capacity. However, increasing the pH beyond 9 resulted in a sharp reduction in the removal of RB 19 from around complete removal at pH 9 to only 91% at pH 12. The reduction of RB 19 removal percent at higher pH might be explained by the formation of OH^- and subsequent competition with the RB 19 molecules for adsorption sites [36,38] on the

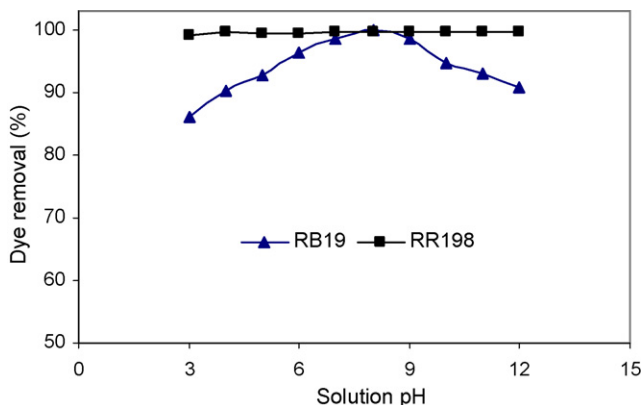


Fig. 3. Effect of initial pH of dye solution on removal of RB 19 and RR 198 (MgO dosage = 0.2 g, initial dye concentration = 100 mg/L, stirring time = 20 min).

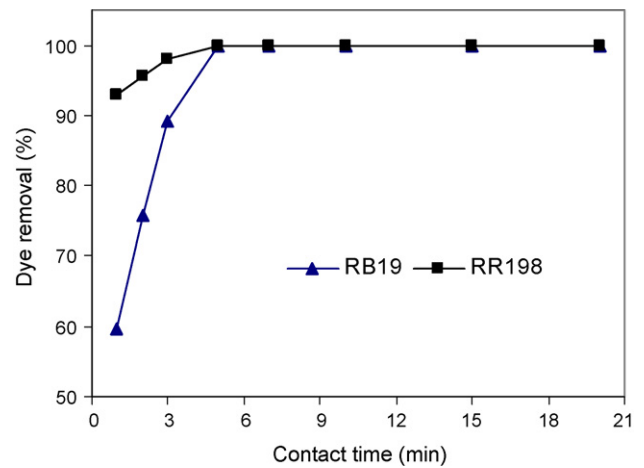


Fig. 4. Effect of stirring time on removal of RB 19 and RR 198 (MgO dosage = 0.2 g, initial dye concentration = 100 mg/L, initial pH 8).

surface of MgO, leading to the reduction of RB 19 removal efficiency.

Based on the trend shown in Fig. 3, the removal of RR 198 was almost independent of pH and stayed higher than 99% over the entire range of the experimental pHs. Hence, no significant effect of pH was observed on the removal of RR 198 using MgO. The independency of RR 198 adsorption from the liquid pH suggests that, in addition to the electrostatic attraction, other adsorption mechanisms such as hydrogen bonding may also be at play [37]. Differences in the adsorption mechanisms of RB 19 and RR 198 on MgO powder can be related to their physicochemical properties and structure. According to the above results, a pH of 8 was chosen as the optimum pH for removal of both dyes in the next experiments.

3.2.3. Effect of contact time

The contact time between adsorbate and adsorbent is the most important design parameter that affects the performance of adsorption processes. The effect of contact or stirring time on the performance of MgO in adsorbing RB 19 and RR19 was investigated individually. The solution pH and MgO dosage were fixed at their obtained optimum values. The initial dye concentrations for all test solutions were 100 mg/L. Fig. 4 shows removal efficiencies for the two dyes as a function of stirring times ranging between 1 and 20 min. These data indicate that adsorption started immediately upon adding the MgO powder to both solutions. The removal efficiency of RB 19 rapidly increased from 60% in the first minute of contact to 100% as the stirring was increased to 5 min, when the equilibrium condition was attained. For RR 198, the percentage of removal obtained in the first minute of stirring was 93%, and complete removal was attained when the stirring was continued to 5 min. Thus, the contact time required to achieve the equilibrium and complete adsorption for both of the tested model dyes was the same. Therefore, the optimum contact time for MgO nanoparticles in the tested dyes was considered to be 5 min. The shorter the contact time in an adsorption system, the lower would be the capital and operational costs for real-world applications. The contact time obtained in this study for equilibrium adsorption onto MgO powder is shorter than most of the reported values for dye adsorption for other adsorbents [6,30,39–41].

3.2.4. Effect of dye concentration

The initial dye concentration is another important variable that can affect the adsorption process. The effect of initial concentration of RB 19 and RR 198 dyes between 50 and 300 mg/L was studied on their adsorption onto MgO powder under previously determined

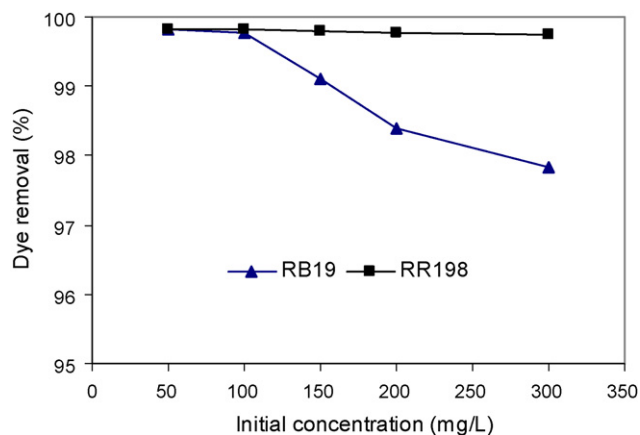


Fig. 5. Effect of initial dye concentration on removal of RB 19 and RR 198 (MgO dosage = 0.2 g, initial pH 8, stirring time = 5 min).

optimum conditions. The results, in terms of removal efficiency versus initial concentration of dye, are indicated in Fig. 5. According to Fig. 5, RB 19 removal slightly decreased from around 100% at a concentration of 50 mg/L to 98% when the concentration was increased to 300 mg/L. In the case of RR 198, the removal efficiency remained constant at greater than 99.8% over the whole range of the investigated dye concentrations, revealing the independency of its adsorption from the initial concentration. This indicates that MgO nanoparticles have greater affinity for RR 198 than RB 19. This is likely due to the higher molecular weight and size of RR 198 as compared to RB 19. Overall, we found that the prepared MgO powder had high adsorption affinities for both RB 19 and RR 198, which are models of anthraquinone and azo class dyes. The adsorption capacity of MgO at the maximum investigated dye concentration was 50 mg/g for each of the tested dyes.

3.3. Adsorption isotherm modeling

The equilibrium adsorption data of RB 19 and RR 198 onto MgO adsorbent was analyzed using Langmuir and Freundlich models. Model fits to equilibrium adsorption results of both dyes were assessed based on the values of the determination coefficient (R^2) of the linear regression plot. The obtained experimental data were fit with these two models; the resulting plots are shown in Fig. 6. Table 2 summarizes the models constants and the determination coefficients. As shown in Table 2, the R^2 of the Langmuir isotherm was greater than that of the Freundlich isotherm for the adsorption of both investigated dyes. This indicates that the adsorption of RB 19 and RR 198 on nano-MgO particles is better described by the Langmuir model than the Freundlich model. This in turn suggests that adsorption occurs as the monolayer dyes adsorb onto the homogenous adsorbent surface. Other researchers have also reported a Langmuir model for the adsorption of RB 19 and RR 198 [42–49]. Table 2 shows that the maximum predictable adsorption capacity of RB 19 and RR 198 are 166.7 and 123.5 mg dye/g MgO, respectively. The dye adsorption process is affected by the properties of both dyes and adsorbent [50]. Due to the steric hindrance associated with the size of the dyes, a higher adsorption capac-

Table 2
Adsorption isotherms parameters of RB 19 and RR 198 onto MgO.

Dye	Langmuir model				Freundlich model			
	q_{max}	b	R^2	ARE	K_F	n	R^2	ARE
RB 19	166.7	0.07	0.998	6.2	12.2	1.9	0.908	11.6
RR 198	123.5	0.94	0.999	6.1	19.9	5.8	0.797	14.8

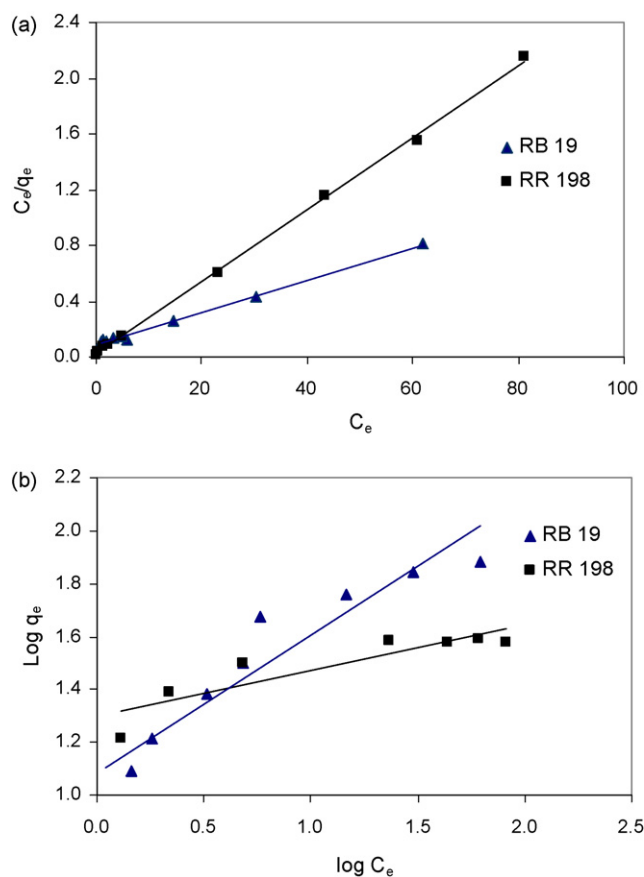


Fig. 6. Isotherm plots of RB 19 and RR 198 adsorption onto MgO nanoparticles: (a) Langmuir isotherm and (b) Freundlich isotherm (MgO dosage = 0.1–1 g, initial pH 8, stirring time = 48 h, initial dye concentration = 100 mg/L).

ity can be achieved for small dye molecules [48] under the same experimental conditions. Owing to the similarity of the adsorbent used in all experiments carried out during this study, the difference in adsorption removal and capacity of RB 19 and RR 198 may be attributed to their chemical structure and properties, particularly the difference in size of the dye molecules.

Table 3 compares the maximum capacity of the homogenous monolayer adsorption of the tested dyes obtained in this work with those reported in the open literature using different materials. As shown in Table 3, the MgO powder had a large adsorption capacity for RB 19 and RR 198 from a dye solution.

From an engineering perspective, obtaining a relatively high adsorption capacity, in addition to a pH-independency for RB 19

Table 3
Comparison of the maximum adsorption capacities of RB 19 and RR 198 onto MgO with other adsorbents.

Dye	Adsorbent	Condition	q_{max}	Reference
RB 19	Nano-MgO	25 °C	166.7	This work
RB 19	Wheat bran	20 °C	97.1	42
RB 19	Zr(IV)-loaded collagen fiber	30 °C	369.1	43
RB 19	Polyethyleneimine	25 °C	121	44
RB 19	Mycelium pellets	20 °C	160	45
RB 19	Fungal biomass	30 °C (pH 2)	80.9	46
RB 19	Modified bentonite	20 °C (pH 2)	207	47
RR 198	Nano-MgO	25 °C	125	This work
RR 198	Sewage sludge char	–	25	48
RR 198	Activated carbon (F400)	–	400	49
RR 198	Activated carbon (C207)	–	123	49
RR 198	Activated carbon (EA207)	–	72	49

Table 4
Adsorption kinetic constants of RB 19 and RR 198 onto MgO.

Dye	$q_{e,exp}$	Pseudo-first-order model			Pseudo-second-order model		
		k_1	$q_{e,cal}$	R^2	k_2	$q_{e,cal}$	R^2
RB 19	50	0.07	43.5	0.874	0.2	49.9	0.999
RR 198	50	0.09	47.9	0.962	0.3	50	1

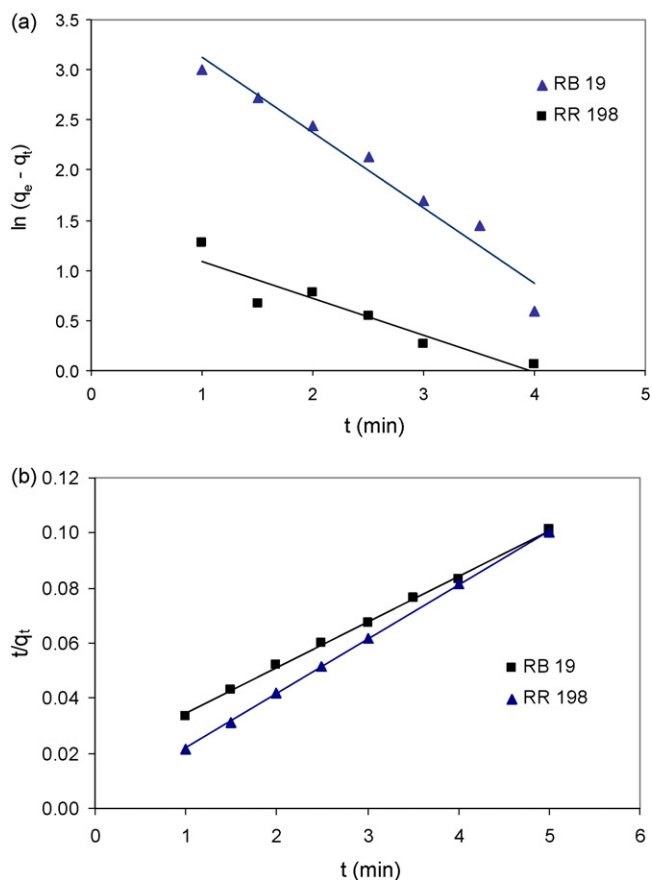


Fig. 7. Plots of first- and second-order rates for adsorption of RB 19 and RR 198 onto MgO nanoparticles: (a) pseudo-first-order rate and (b) pseudo-second-order rate.

adsorption and alkaline optimum adsorption pH for RR 198, as well as the short contact time required, present the prepared nano-MgO powder as an attractive and promising alternative for both azo and anthraquinone dye removal in practical applications.

The goodness of fit for the models used to predict the adsorption of RB 19 and RR198 was further confirmed by the average relative error (ARE) factor between the experimental data and the model estimates of adsorption capacities. ARE can be determined by the following expression [38]:

$$ARE(\%) = \frac{100}{n} \sum_i^n \left| \frac{q_{i,est} - q_{i,exp}}{q_{i,exp}} \right|$$

where $q_{i,exp}$ and $q_{i,est}$ are the experimental and estimated adsorption capacities, respectively, and n represents the number of the tests. The values of ARE for the Langmuir and Freundlich models are given in Table 2. As shown, for both dyes the values of ARE in Langmuir is lower than that of Freundlich model, confirming the better fit of the Langmuir model to the experimental data.

The favorability of the RB 19 and RR 198 adsorption process onto MgO was evaluated using a dimensionless parameter (R_L) derived

from the Langmuir expression. It is defined as follows:

$$R_L = \frac{1}{1 + bC_i}$$

The adsorption process can be defined as irreversible ($R_L = 0$), favorable ($0 < R_L < 1$), linear ($R_L = 1$) or unfavorable ($R_L > 1$) in terms of R_L [51]. The calculated values of R_L for adsorption of RB 19 and RR 198 fall between 0 and 1, thus the adsorption of both RB 19 and RR 198 onto MgO is favorable.

3.4. Adsorption kinetic modeling

To describe the adsorption behavior and rate, the data obtained from adsorption kinetic experiments were evaluated using pseudo-first- and pseudo-second-order reaction rate models. Plots of experimental results of the two model dyes fitted to the selected adsorption models are shown in Fig. 7. Table 4 gives a summary of the models and constants along with the determination coefficients for the linear regression plots of both tested dyes. As shown in Table 4, higher values of R^2 were obtained for pseudo-second-order than for pseudo-first-order adsorption rate models, indicating that the adsorption rates of RB 19 and RR 198 onto the MgO nanoparticles can be more appropriately described using the pseudo-second-order rate rather than pseudo-first-order rate. No kinetic model was found in the scientific literature for the adsorption of either RB 19 or RR 198 from aqueous solution for comparison.

4. Conclusion

In this study, a nanoparticle MgO powder was produced and tested as a novel adsorbent for the removal of azo and anthraquinone dyes. The effects of MgO dosage, initial pH, contact time and initial dye concentration on the removal of RB 19 and RR 198 were investigated separately through batch experiments. Results indicated that the synthesized powder could effectively remove high concentrations of azo and anthraquinone model dyes in a short contact time. The optimum dosage, pH and contact time were obtained to be 0.2 g, pH 8 and 5 min, respectively. Isotherm modeling revealed that the Langmuir equation could better describe the adsorption of both dyes onto the MgO as compared to other models. Kinetic data were appropriately fitted with the pseudo-second-order adsorption rates. Because of the high specific surface area and nano-scale particle size, MgO indicated favorable adsorption behavior for both RB 19 and RR 198. MgO is a non-toxic material and can be made in a simple and cost-effective way for simple application. These unique features present MgO as a novel, promising and feasible alternative for dye removal.

Acknowledgements

The authors gratefully acknowledge the financial and technical support provided by the Tarbiat Modares University, Tehran, Iran.

References

- [1] G. McMullan, C. Meehan, A. Conneely, N. Kirby, T. Robinson, P. Nigam, I.M. Banat, R. Marchant, W.F. Smyth, Microbial decolourisation and degradation of textile dyes, *Appl. Microbiol. Biotechnol.* 56 (2001) 81–87.
- [2] C.I. Pearce, J.R. Lloyd, J.T. Guthrie, The removal of colour from textile wastewater using whole bacterial cells: a review, *Dyes Pigments* 58 (2003) 179–196.

- [3] E.Y. Ozmen, M. Sezgin, A. Yilmaz, M. Yilmaz, Synthesis of β -cyclodextrin and starch based polymers for sorption of azo dyes from aqueous solutions, *Biore-sour. Technol.* 99 (2008) 526–531.
- [4] R. Christie, *Colour Chemistry*, The Royal Society of Chemistry, Cambridge, United Kingdom, 2001.
- [5] G. Crini, Non-conventional low-cost adsorbents for dye removal: a review, *Biore-sour. Technol.* 97 (2006) 1061–1085.
- [6] P. Pengthamkeerati, T. Satapanajaru, O. Singchan, Sorption of reactive dye from aqueous solution on biomass fly ash, *J. Hazard. Mater.* 153 (2008) 1149–1156.
- [7] C. O'Neill, F.R. Hawkes, D.L. Hawkes, N.D. Lourenço, H.M. Pinheiro, W. Delée, Color in textile effluents-sources, measurement, discharge consents and simulation: a review, *J. Chem. Technol. Biotechnol.* 74 (1999) 1009–1018.
- [8] I. Arslan-Alaton, B.H. Gursoy, J.-E. Schmidt, Advanced oxidation of acid and reactive dyes: effect of Fenton treatment on aerobic, anoxic and anaerobic processes, *Dyes Pigments* 78 (2008) 117–130.
- [9] K. Vijayaraghavan, Y.-S. Yun, Bacterial biosorbents and biosorption, *Biotechnol. Adv.* 26 (2008) 266–291.
- [10] F.-C. Wu, R.-L. Tseng, High adsorption capacity NaOH-activated carbon for dye removal from aqueous solution, *J. Hazard. Mater.* 152 (2008) 1256–1267.
- [11] R. Han, D. Ding, Y. Xu, W. Zou, Y. Wang, Y. Li, L. Zou, Use of rice husk for the adsorption of congo red from aqueous solution in column mode, *Biore-sour. Technol.* 99 (2008) 2938–2946.
- [12] Z. Aksu, Application of biosorption for the removal of organic pollutants: a review, *Process Biochem.* 40 (2005) 997–1026.
- [13] S. Karcher, A. Kornmuller, M. Jekel, Screening of commercial sorbents for the removal of reactive dyes, *Dyes Pigments* 51 (2001) 111–125.
- [14] V.J.P. Vilar, C.M.S. Botelho, R.A.R. Boaventura, Methylene blue adsorption by algal biomass based materials: biosorbents characterization and process behaviour, *J. Hazard. Mater.* 147 (2007) 120–132.
- [15] M. Dias, M.C.M. Alvim-Ferraz, M.F. Almeida, J. Rivera-Utrilla, M. Sánchez-Polo, Waste materials for activated carbon preparation and its use in aqueous-phase treatment: a review, *J. Environ. Manage.* 85 (2007) 833–846.
- [16] B. Nagappa, G.T. Chandrappa, Mesoporous nanocrystalline magnesium oxide for environmental remediation, *Micropor. Mesopor. Mater.* 106 (2007) 212–218.
- [17] B. Neppolian, Q. Wang, H. Jung, H. Choi, Ultrasonic-assisted sol-gel method of preparation of TiO_2 nano-particles: characterization, properties and 4-chlorophenol removal application, *Ultrason. Sonochem.* 15 (2008) 649–658.
- [18] G. Zelmanov, R. Semiat, Iron (3) oxide-based nanoparticles as catalysts in advanced organic aqueous oxidation, *Water Res.* 42 (2008) 492–498.
- [19] Z.G. Hu, J. Zhang, W.L. Chan, Y.S. Szeto, The sorption of acid dye onto chitosan nanoparticles, *Polymer* 47 (2006) 5838–5842.
- [20] H.-Y. Shu, M.-C. Chang, H.-H. Yu, W.-H. Chen, Reduction of an azo dye Acid Black 24 solution using synthesized nanoscale zerovalent iron particles, *J. Colloid Interf. Sci.* 314 (2007) 89–97.
- [21] W.L. Du, Z.R. Xu, X.Y. Han, Y.L. Xu, Z.G. Miao, Preparation, characterization and adsorption properties of chitosan nanoparticles for eosin Y as a model anionic dye, *J. Hazard. Mater.* 153 (2008) 152–156.
- [22] I.V. Mishakov, A.F. Bedilo, R.M. Richards, V.V. Chesnokov, A.M. Volodin, V.I. Zaikovskii, R.A. Buyanov, K.J. Klabunde, Nanocrystalline MgO as a dehydrohalogenation, *J. Catal.* 206 (2002) 40–48.
- [23] R. Richards, R.S. Mulukutla, I. Mishakov, V. Chesnokov, A. Volodin, V. Zaikovskii, N. Sun, K.J. Klabunde, Nanocrystalline ultra high surface area magnesium oxide as a selective based catalyst, *Scripta Mater.* 44 (2001) 1663–1666.
- [24] J.C. Crittenden, R.R. Trussell, D.W. Hand, K.J. Howe, G. Tchobanoglous, *Water Treatment: Principles and Design*, 2nd edition, MWH, John Wiley and Sons, Inc., 2005.
- [25] M.A. Aramendía, V. Borau, C. Jiménez, J.M. Marinas, J.R. Ruiz, F.J. Urbano, Influence of the preparation method on the structural and surface properties of various magnesium oxides and their catalytic activity in the Meerwein-Ponndorf-Verley reaction, *Appl. Catal. A: Gen.* 244 (2003) 207–215.
- [26] C. Henrist, J.P. Mathieu, C. Vogels, A. Rulmont, R. Cloots, Morphological study of magnesium hydroxide nanoparticles precipitated in dilute aqueous solution, *J. Cryst. Growth* 249 (2003) 321–330.
- [27] Q. Zhou, J.-W. Yang, Y.-Z. Wang, Y.-H. Wu, D.-Z. Wang, Preparation of nano-MgO/Carbon composites from sucrose-assisted synthesis for highly efficient dehydrochlorination process, *Mater. Lett.* 62 (2008) 1887–1889.
- [28] E. Erdem, G. Çölgeçen, R. Donat, The removal of textile dyes by diatomite earth, *J. Colloid Interf. Sci.* 282 (2005) 314–319.
- [29] R.D. Letterman, *Water Quality and Treatment*, 5th edition, McGraw-Hill, Inc., 1999.
- [30] I.A.W. Tan, A.L. Ahmad, B.H. Hameed, Adsorption of basic dye on high-surface-area activated carbon prepared from coconut husk: equilibrium, kinetic and thermodynamic studies, *J. Hazard. Mater.* 154 (2008) 337–346.
- [31] I. Langmuir, The adsorption of gases on plane surfaces of glass, mica and platinum, *J. Am. Chem. Soc.* 40 (1918) 1361–1403.
- [32] H.M.F. Freundlich, Over the adsorption in solution, *J. Phys. Chem.-US* 57 (1906) 385–471.
- [33] S.C.R. Santos, V.J.P. Vilar, R.A.R. Boaventura, Waste metal hydroxide sludge as adsorbent for a reactive dye, *J. Hazard. Mater.* 153 (2008) 999–1008.
- [34] Y.S. Ho, G. McKay, Pseudo-second-order model for sorption processes, *Process Biochem.* 34 (1999) 451–465.
- [35] M.A. Aramendía, J.A. Benítez, V. Borau, C. Jiménez, J.M. Marinas, J.R. Ruiz, F. Urbano, Characterization of various magnesium oxides by XRD and ^1H MAS NMR spectroscopy, *J. Solid State Chem.* 144 (1999) 25–29.
- [36] X. Wang, N. Zhu, B. Yin, Preparation of sludge-based activated carbon and its application in dye wastewater treatment, *J. Hazard. Mater.* 153 (2008) 22–27.
- [37] Y.S. Al-Degs, M.I. El-Barghouthi, A.H. El-Sheikh, G.M. Walker, Effect of solution pH, ionic strength, and temperature on adsorption behavior of reactive dyes on activated carbon, *Dyes Pigments* 77 (2008) 16–23.
- [38] F.A. Pavan, S.L.P. Dias, E.C. Lima, E.V. Benvenuti, Removal of Congo red from aqueous solution by anilinepropylsilica xerogel, *Dyes Pigments* 76 (2008) 64–69.
- [39] B.H. Hameed, M.I. El-Khaiary, Batch removal of malachite green from aqueous solutions by adsorption on oil palm trunk fibre: equilibrium isotherms and kinetic studies, *J. Hazard. Mater.* 154 (2008) 237–244.
- [40] R. Jain, S. Sikarwar, Removal of hazardous dye congo red from waste material, *J. Hazard. Mater.* 152 (2008) 942–948.
- [41] A. Olgun, N. Atar, Equilibrium and kinetic adsorption study of Basic Yellow 28 and Basic Red 46 by a boron industry waste, *J. Hazard. Mater.* 161 (2009) 148–156.
- [42] F. Çiçek, D. Özer, A. Özer, A. Özer, Low cost removal of reactive dyes using wheat bran, *J. Hazard. Mater.* 146 (2007) 408–416.
- [43] Y. Gu, X. Liao, Y. Wang, B. Shi, Adsorption of dyes on Zr(IV)-loaded collagen fiber from aqueous solution, *J. Basic Sci. Eng.* 15 (2007) 414–423.
- [44] M.H. Liao, W.C. Chen, W.C. Lai, Magnetic nanoparticles assisted low-molecular-weight polyethyleneimine for fast and effective removal of reactive blue 19, *Fresen. Environ. Bull.* 15 (2006) 609–613.
- [45] S.J. Zhang, M. Yang, Q.X. Yang, Y. Zhang, B.P. Xin, F. Pan, Biosorption of reactive dyes by the mycelium pellets of a new isolate of *Penicillium oxalicum*, *Biotechnol. Lett.* 25 (2003) 1479–1482.
- [46] M. Iqbal, A. Saeed, Biosorption of reactive dye by loofa sponge-immobilized fungal biomass of *Phanerochaete chrysosporium*, *Process Biochem.* 42 (2007) 1160–1164.
- [47] A. Özcan, Ç. Ömeroğlu, Y. Erdoğan, A.S. Özcan, Modification of bentonite with a cationic surfactant: an adsorption study of textile dye Reactive Blue 19, *J. Hazard. Mater.* 140 (2007) 173–179.
- [48] C. Jindarom, V. Meeyoo, B. Kitiyanan, T. Rirksomboon, P. Rangsunvigit, Surface characterization and dye adsorptive capacities of char obtained from pyrolysis/gasification of sewage sludge, *Chem. Eng. J.* 133 (2007) 239–246.
- [49] S.J. Allen, B. Koumanova, Decolourisation of water/wastewater using adsorption: review, *J. Univ. Chem. Technol. Met. (Sofia)* 40 (2005) 175–192.
- [50] V. Rocher, J.-M. Siaugue, V. Cabuil, A. Bee, Removal of organic dyes by magnetic alginate beads, *Water Res.* 42 (2008) 1290–1298.
- [51] R. Sivaraj, C. Namasivayam, K. Kadirvelu, Orange peel as an adsorbent in the removal of acid violet 17 (acid dye) from aqueous solutions, *Waste Manage.* 21 (2001) 105–110.